Stability Characteristics of Non-Darcy Three-Component Marangoni Convection with Combined Dufour and Magnetic Effects in a Two-Layer Composite System

[1*]Shivaraja. J. M., [2]Manasa. K V, [3]Sushmitha. S V, [4]Naveen Kumar. K S, [5] Madhulatha M, [6]Anushree. M N

[1*] Faculty, Department of Mathematics, Suvarna Gange Campus, Mangasandra, Bengaluru North University, Tamaka, Kolar

[2,3,4,5&6] PG Mathematics students, Suvarna Gange Campus, Mangasandra, Bengaluru North University, Tamaka, Kolar

[*]Corresponding Author

DOI: https://doi.org/10.51584/IJRIAS.2026.11070096

Received: 22 July 2026; Accepted: 27 July 2026; Published: 05 August 2026

ABSTRACT

The stability characteristics of non-Darcy three-component Marangoni convection with combined Dufour and magnetic effects in a two-layer composite system are investigated analytically using a modified Darcy–Brinkman formulation. The system consists of an upper electrically conducting fluid layer overlying a porous layer saturated with the same fluid. The upper boundary is free and deformable, with surface tension depending on temperature and the concentrations of two solute species, while the lower boundary is rigid. The basic state is quiescent, and the Boussinesq approximation is employed. The governing momentum, energy, species-transport, and magnetic-induction equations are linearized about the basic state and reduced, by normal-mode analysis, to a coupled ordinary differential eigenvalue problem. The Dufour effect is incorporated in the energy equations to represent diffusion–thermal coupling, while magnetic damping is represented through the Chandrasekhar parameters of the fluid and porous layers. Continuity of normal velocity, stress, temperature, concentration, heat flux, and mass flux is imposed at the fluid–porous interface, together with the appropriate free-surface Marangoni conditions. An exact solution procedure is used to obtain the velocity, temperature, and concentration disturbance fields, and the thermal Marangoni number is determined from the remaining coupled surface condition. The effects of wave number, Darcy number, Dufour parameter, diffusivity ratios, solutal Marangoni numbers, and magnetic parameters are examined. The results show that magnetic fields generally stabilize the system, whereas increased permeability and stronger solutal Marangoni driving can promote instability. The Dufour effect modifies the stability threshold through thermal–solutal cross-diffusion, and the two solutal components introduce additional competing transport mechanisms that are absent in double-diffusive models. The present formulation provides a unified framework for assessing the combined influence of non-Darcy resistance, triple diffusion, thermocapillarity, cross-diffusion, and magnetic damping in layered composite systems.

Key words: Non-Darcy convection, Three-component Marangoni convection, Dufour effect, Magneto hydrodynamics, Two-layer composite system, Triple diffusive convection, Porous medium, Diffusion-thermal (Dufour) effect.

INTRODUCTION

Three-component convection arises when temperature and two independent concentration fields diffuse at different rates and interact through buoyancy, interfacial tension, or both. Such systems occur in multicomponent materials processing, crystal growth, geothermal transport, chemical engineering, and thermal management. Marangoni convection is generated by gradients of surface tension along a free interface and is particularly sensitive to the coupled evolution of temperature and concentration fields. When a fluid layer is coupled to a porous layer, the instability mechanism is further modified by permeability, viscous and inertial resistance, and interfacial transmission conditions. The introduction of a magnetic field adds Lorentz-force damping in electrically conducting fluids, while the Dufour effect couples concentration gradients to heat transport. The resulting problem therefore contains several interacting stabilizing and destabilizing mechanisms that cannot be represented by a single-diffusion or conventional Darcy model.

Research gap and novelty. The main contribution of the present study is the simultaneous treatment of five coupled mechanisms within one stability framework: (i) non-Darcy flow resistance in the porous layer, (ii) thermocapillary forcing at a free upper boundary, (iii) two independent solutal fields with distinct diffusivities, (iv) Dufour diffusion–thermal coupling, and (v) magnetic damping in both the fluid and porous regions. In contrast to models that isolate only one or two of these mechanisms, the present formulation permits their combined influence on the critical thermal Marangoni number to be assessed using a common set of dimensionless parameters. This is relevant to applications in which permeable substrates, multicomponent mixtures, electromagnetic control, and cross-diffusion occur simultaneously. The novelty therefore lies not only in adding individual physical effects, but in quantifying their coupled influence on the stability threshold of a two-layer composite system.

Considerable attention has been devoted to the study of Marangoni convection with Dufour and magnetic effects in various configurations such as boundary layer flows, fluid layers, and porous media. However, the stability characteristics of Non-Darcy three-component Marangoni convection with combined Dufour and magnetic effects in a two-layer composite system remain an important area of investigation due to their relevance in crystal growth, material processing, geothermal systems, and chemical engineering applications.

Interfacial convection in fluid–porous composite systems has been widely studied due to its importance in crystal growth, geothermal systems, chemical reactors, and thermal management technologies. In particular, Marangoni convection driven by surface tension gradients continues to attract significant attention when coupled with double and triple diffusive transport processes. Nield & Bejan (2017) provided a comprehensive foundation on convection in porous media, highlighting how Darcy and non-Darcy models govern flow behavior in porous structures. Their work established the significance of permeability and inertial effects in stability analysis of layered systems. Siddheshwar et al. (2019) investigated thermosolutal Marangoni convection and showed that surface tension variations due to both temperature and concentration significantly influence instability thresholds in fluid layers. Bhadauria & Agarwal (2020) analyzed double diffusive convection in porous media and demonstrated that competing thermal and solutal gradients can either stabilize or destabilize the system depending on diffusivity ratios. Pranesh & Kiran (2020) extended the study to magnetohydrodynamic (MHD) convection and observed that the application of a magnetic field suppresses velocity fluctuations due to Lorentz force effects. Rionero (2021) studied stability in composite fluid–porous systems and emphasized the importance of interface conditions in determining critical Rayleigh and Marangoni numbers. Ghosh & Mukherjee (2021) examined non-Darcy convection models and found that inertial effects significantly modify the onset of convection in high-permeability porous layers. Kuznetsov (2022) focused on triple-diffusive convection systems and showed that interaction among thermal, solutal, and nanoparticle concentration fields leads to complex instability behavior. Abdelkhalek & Chamkha (2023**)** investigated Marangoni convection in porous media with magnetic fields and reported that increasing Hartmann number delays the onset of instability. Zhao et al. (2024) studied Dufour and Soret effects in multi-component convection and found strong coupling between heat and mass transfer significantly alters stability boundaries.

Mathematical modeling

The physical model under the consideration of composite layer system with a horizontal two – component fluid saturated, incompressible, isotropic and sparsely packed porous layer is of thickness d_{mj} and a fluid layer of thicknessd_{fj}. Both the boundaries of the composite layer system are considered to be rigid and these boundaries are acts like heat and mass insulators along with maintained, distinct concentration and temperature. The origin point of the Cartesian coordinate system is taken exactly at the intersection of porous and fluid layer along with direction of z – axis is vertically upwards. In addition to that, for the effect of

ISSN No. 2454-6194 | DOI: 10.51584/IJRIAS |Volume XI Issue VII July 2026

density variation, Boussinesq approximation is included. Under these following assumptions, the governing equations are, the continuity, momentum, temperature and concentration equations as follows.

For fluid layer,

Continuity Equation :

$$\nabla_{fj} \cdot \overrightarrow{q_{fj}} = 0 \tag{1}$$

Solenoidal Property of the Magnetic Field:

$$\nabla_{fj} \cdot \vec{H}_{fj} = 0 \tag{2}$$

Momentum Equation :

$$\rho_{0fj}\left[\frac{\partial \overrightarrow{q_{fj}}}{\partial t_{fj}} + (\overrightarrow{q_{fj}} \cdot \nabla_{fj})\overrightarrow{q_{fj}}\right] = -\nabla_{fj}P_{fj} + \mu_{fj}\,{\nabla_{fj}}^2\,\overrightarrow{q_{fj}} + \mu_{fp}(\vec{H}_{fj} \cdot \nabla_{fj}) \tag{3}$$

Energy Equation :

$$\frac{\partial T_{fj}}{\partial t_{fj}} + (\overrightarrow{q_{fj}} \cdot \nabla_{fj})T_{fj} = k_{fj}\,\nabla_{fj}^2\,T_{fj} + k_{Tfj}\,\nabla_{fj}^2\,c_{fj} \tag{4}$$

Concentration Equation for Species 1:

$$\frac{\partial c_{1fj}}{\partial t_{fj}} + (\overrightarrow{q_{fj}} \cdot \nabla_{fj})c_{1fj} = k_{fj1}\,{\nabla^2}_{fj}\,c_{1fj} \tag{5}$$

Concentration Equation for Species 2:

$$\frac{\partial c_{2fj}}{\partial t_{fj}} + (\overrightarrow{q_{fj}} \cdot \nabla_{fj})c_{2fj} = k_{fj2}\,{\nabla^2}_{fj}\,c_{2fj} \tag{6}$$

Equation of Magnetic Induction Equation:

$$\frac{\partial \vec{H}_{fj}}{\partial t_{fj}} = \nabla_{fj} \times \overrightarrow{q_{fj}} \times \vec{H}_{fj} + v_{fj}{\nabla^2}_{fj}\,\vec{H}_{fj} \tag{7}$$

For porous layer,

Continuity Equation :

$$\nabla_{mj} \cdot \overrightarrow{q_{mj}} = 0 \tag{8}$$

Solenoidal Property of the Magnetic Field:

$$\nabla_{mj} \cdot \vec{H}_{mj} = 0 \tag{9}$$

Momentum Equation:

$$\left(\frac{\rho_{0mj}}{\phi_{mj}}\right)\frac{\partial \overrightarrow{q_{mj}}}{\partial t_{mj}} = -\nabla_{mj}\,p_{mj} - \left(\frac{\mu_{mj}}{K_{mj}}\right)\overrightarrow{q_{mj}} + \mu_{mj}\nabla_{mj}^2\,\overrightarrow{q_{mj}} + \mu_{mp}(\vec{H}_{mj} \cdot \nabla_{mj}) \tag{10}$$

ISSN No. 2454-6194 | DOI: 10.51584/IJRIAS |Volume XI Issue VII July 2026

Energy Equation :

$$A_{mj}\frac{\partial T_{mj}}{\partial t_{mj}}+\left(\overrightarrow{q_{\mathrm{mj}}}\cdot\nabla_{mj}\right)T_{mj}=k_{mj}\nabla_{mj}^{2}T_{mj}+k_{Tmj}\nabla_{mj}^{2}c_{mj} \tag{11}$$

Concentration Equation for Species-1 :

$$\phi_{mj}\frac{\partial \mathrm{c}_{1\mathrm{mj}}}{\partial t_{mj}}+\left(\overrightarrow{q_{\mathrm{mj}}}\cdot\nabla_{mj}\right)\mathrm{c}_{1\mathrm{mj}}=k_{mj1}\nabla_{mj}^{2}c_{1mj} \tag{12}$$

Concentration Equation for Species-2 :

$$\phi_{mj}\frac{\partial \mathrm{c}_{2\mathrm{mj}}}{\partial t_{mj}}+\left(\overrightarrow{q_{\mathrm{mj}}}\cdot\nabla_{mj}\right)\mathrm{c}_{2\mathrm{mj}}=k_{mj2}\nabla_{mj}^{2}c_{2mj} \tag{13}$$

Equation of Magnetic Induction Equation:

$$\frac{\partial \vec{H}_{mj}}{\partial t_{mj}}=\nabla_{mj}\times\overrightarrow{q_{\mathrm{mj}}}\times\vec{H}_{mj}+v_{mj}\nabla_{mj}^{2}\vec{H}_{mj} \tag{14}$$

Notations:

- $\overrightarrow{q_{\mathrm{fj}}}=\left(u_{fj},\ v_{fj},\ w_{fj}\right)$: velocity vector in the fluid layer
- $\overrightarrow{q_{\mathrm{mj}}}=\left(u_{mj},\ v_{mj},\ w_{mj}\right)$: velocity vector in the porous layer
- t_{fj}, t_{mj}:time
- P_{fj}, P_{mj}: pressures in the fluid and porous layers
- ρ_{0fj}: reference fluid density
- ρ_{fj}, ρ_{mj}: fluid and porous layer densities
- $\mu_{fj},\ \mu_{mj}$: dynamic viscosities in the fluid and porous layers
- $T_{fj},\ T_{mj}$: temperatures in the fluid and porous layers
- C_{fj}, C_{mj}: solute concentrations in the fluid and porous layers
- $k_{fj},\ \kappa_{mj}$: thermal diffusivities in the fluid and porous layers
- k_{fj1} , k_{mj1} : solutal-1 diffusivities in the fluid and porous layers
- k_{fj2} , k_{mj2} : solutal-2 diffusivities in the fluid and porous layers
- k_{Tfj} , k_{Tmj}: Dufour coefficients in the fluid and porous layers
- H_{fj}, H_{mj}: magnetic field in the fluid and porous layer
- μ_{fp}, μ_{mp}: magnetic permeability in the fluid and porous layers
- α_T: thermal expansion coefficient

ISSN No. 2454-6194 | DOI: 10.51584/IJRIAS |Volume XI Issue VII July 2026

- α_c: solutal expansion coefficient
- $\emptyset_{mj}$: porosity of the porous medium
- K_{mj} permeability of the porous medium
- $A_{mj} = \frac{(\rho_0 c_p)_m}{(\rho c_p)_f}$: ratio of heat capacities
- c_p: Specific heat
- $P_{fj} = p_{fj} + \frac{\mu_{pj} H_{fj}^2}{2}$:total pressure
- $v_{fj} = \frac{1}{\mu_p \sigma}$: magnetic viscosity
- $v_{mj} = \frac{v_f}{\emptyset}$: effective magnetic viscosity in the porous medium

Stability Analysis

To examine the stability of the conductive basic state, the unperturbed composite system is assumed to be motionless. Thus, the basic velocities in both layers are zero, and heat and mass transfer occur only by conduction and diffusion. The basic temperature and concentration profiles are obtained from the steady one-dimensional transport equations subject to the prescribed boundary and interface conditions. These profiles are then perturbed by infinitesimal disturbances in velocity, pressure, temperature, and the two concentration fields.

For the fluid layer, basic state is mathematically represented as follows:

$$\left[\overrightarrow{q_{\mathrm{fj}}}, p_{fj}, T_{fj}, c_{1fj}, c_{2fj}, H_{fj}\right] = \left[0, p_{fjb}(z_{fj}), T_{fjb}(z_{fj}), c_{1fjb}(z_{fj}), c_{2fjb}(z_{fj}), H_{fjb}(z_{fj})\right]$$

For the porous layer, basic state is mathematically represented as follows:

$$\left[\overrightarrow{q_{\mathrm{mj}}}, p_{mj}, T_{mj}, c_{1mj}, c_{2mj}, H_{mj}\right] = \left[\,0, p_{mjb}(z_{mj}), T_{mjb}(z_{mj}), c_{1mjb}(z_{mj}), c_{2mjb}(z_{mj}), H_{mjb}(z_{mj})\right]$$

For both fluid and porous layer, the temperature distribution and concentration distributions are $T_{fjb}(z_{fj})$, $T_{mjb}(z_{mj})$and $C_{fjb}(z_{fj})$,$C_{mjb}(z_{mj})$ respectively are mentioned in below table.

Distributions	Fluid layer	Porous layer
Temperature distribution	$T_{fjb}(z_{fj}) = T_0 + \left(\frac{(T_u - T_0)}{d_{fj}}\right) z_{fj}$	$T_{mjb}(z_{mj}) = T_0 + \left(\frac{(T_0 - T_L)}{d_{mj}}\right) z_{mj}$
Species-1 distribution	$C_{1fjb}(z_{fj}) = C_{1fj0} + \left(\frac{(C_{1fju} - C_{1fj0})}{d_{fj}}\right) z_{fj}$	$C_{1mjb}(z_{mj}) = C_{1mj0} + \left(\frac{(C_{1mj0} - C_{1mjL})}{d_{\mathrm{mj}}}\right) z_{mj}$
Species-2 distribution	$C_{2fjb}(z_{fj}) = C_{2fj0} + \left(\frac{(C_{2fju} - C_{2fj0})}{d_{fj}}\right) z_{fj}$	$C_{1mjb}(z_{mj}) = C_{2mj0} + \left(\frac{(C_{2mj0} - C_{2mjL})}{d_{\mathrm{mj}}}\right) z_{mj}$

Where

ISSN No. 2454-6194 | DOI: 10.51584/IJRIAS |Volume XI Issue VII July 2026

$$T_0 = \left\{ \begin{array}{c} \dfrac{k_{fj}\, d_{mj} T_u + d\, k_{mj}\, T_L}{k_{fj}\, d_{mj} + d_{fj}\ k_{mj}} + \dfrac{d_{mj}\, k_{fjT}\, C_{1fju} + k\, T_m\, d\, C_{1mjl}}{k_{fj}\, d_{mj} + d_{fj}\ k_{mj}} \\ -C_{1fj0}\left(\dfrac{d_{fj}\, k_{fj}\ T_{mj} + d_{mj}\, k_{fjT}}{k_{fj}\, d_{mj} + d_{fj}\, k_{mj}}\right) - C_{2fj0}\left(\dfrac{d_{fj}\, k_{fj}\ T_{mj} + d_{mj}\, k_{fjT}}{k_{fj}\, d_{mj} + d_{fj}\, k_{mj}}\right) \end{array} \right\}$$

$$C_{1fj0} = \frac{k_{mj}\, C_{1fju} d_{mj} + d_{fj}\, k_{mj1}\, C_{1mjL}}{d_{fj}\, k_{mj1} + d_{mj}\, k_{mj}}$$

$$C_{2fj0} = \frac{k_{mj}\, C_{2fju} d_{mj} + d_{fj}\, k_{mj2}\, C_{2mjL}}{d_{fj}\, k_{mj2} + d_{mj}\, k_{mj}}$$

are the interface temperature and concentrations respectively. To analyse the stability of the basic state solution, an infinitesimal perturbations are introduced and the perturbed quantities are of the form.

For fluid layer

$$\left[\overrightarrow{q_{fj}}, P_{fj}, T_{fj}, c_{1fj}, c_{2fj}, \overrightarrow{H_{fj}}\,\right] = \left\{ \begin{array}{r} \left[\,0,\ P_{fjb}(z_{fj}), T_{fjb}(z_{fj}), C_{1fjb}(z_{fj}), C_{2fjb}(z_{fj}), \overrightarrow{H_{fjb}}\right] \\ +\ \left[\overrightarrow{q_{fj}}', P'_{fj}, \theta'_{fj}, S'_{1fj}, S'_{2fj}, \overrightarrow{H_{fj}}'\,\right] \end{array} \right\}$$

For porous layer

$$\left[\overrightarrow{q_{mj}}, P_{mj}, T_{mj}, c_{1mj}, c_{2mj}, \overrightarrow{H_{mj}}\,\right] = \left\{ \begin{array}{r} \left[\,0,\ P_{mjb}(z_{mj}), T_{mjb}(z_{mj}), C_{1mjb}(z_{mj}), C_{2mjb}(z_{mj}), \overrightarrow{H_{mjb}}\right] \\ +\ \left[\overrightarrow{q_{mj}}', P'_{mj}, \theta'_{mj}, S'_{1mj}, S'_{2mj}, \overrightarrow{H_{mj}}'\,\right] \end{array} \right\}$$

Substitute above perturbations into equations $(1)-(14)$ and apply two times curl on the momentum equations to eliminate the pressure term. The resulting equations are linearized for $(1)-(14)$, then they are non-dimensionalised using the following variables $\frac{{d_{fj}}^2}{k_{fj}}$, $\frac{k_{fj}}{d_{fj}}$, $C_{1fju} - C_{1fj0}$, $C_{2fju} - C_{2fj0}$, d_{fj} and $T_0 - T_U$, for time, velocity, species-1, species-2, length and temperature respectively in region – 1 and $\frac{d_m^2}{k_m}$, $\frac{k_m}{d_m}$, $C_{1mj0} - C_{1mjL}$, d_m, $C_{2mj0} - C_{2mjL}$, and $T_L - T_0$ are the corresponding scale factors in region – 2. Applying normal mode expansions to the perturbed non-dimensionalised quantities result in the following ordinary differential equations,

For Fluid layer,

$$\left(D_{fj}^2 - a_{\mathrm{fj}}^2\right)^2 W_{fj} = Q_{fj} {D^2}_{fj} W_{fj} \tag{15}$$

$$\left(D_{fj}^2 - a_{\mathrm{fj}}^2\right)\Theta_{fj} + W_{fj} f(z_{fj}) + \mathrm{d_{uf}}\left(D_{fj}^2 - a_{\mathrm{fj}}^2\right) S_{1fj} = 0 \tag{16}$$

$$\tau_{1fj}\left(D_{fj}^2 - a_{\mathrm{fj}}^2\right) S_{1fj} + W_{fj} = 0 \tag{17}$$

$$\tau_{2fj}\left(D_{fj}^2 - a_{\mathrm{fj}}^2\right) S_{2fj} + W_{fj} = 0 \tag{18}$$

For Porous layer,

$$\left[\hat{\mu}\, {\beta^2}_{mj}\left(D_{mj}^2 - a_{mj}^2\right) - 1\right]\left(D_{mj}^2 - a_{mj}^2\right) W_{mj} = 0 \tag{19}$$

$$\left(D_{mj}^2 - a_{mj}^2\right)\Theta_{mj} + W_{mj}\, g_{mj}(z_{mj}) + d_{um}\left(D_{mj}^2 - a_{mj}^2\right) S_{1mj} = 0 \tag{20}$$

$$\tau_{1mj}\left(D_{mj}^2 - a_{mj}^2\right) S_{1mj} + W_{mj} = 0 \tag{21}$$

$$\tau_{2mj}\left(D_{mj}^2-a_{mj}^2\right)S_{2mj}+W_{mj}=0 \tag{22}$$

Where, for fluid layer, $p_r=\frac{\nu}{k_{fj}}$ is the Prandtl number, $\tau_{1fj}=\frac{k_{1fj}}{k_{fj}}$ is the ratio of species-1 diffusivity to thermal diffusivity, $\tau_{2fj}=\frac{k_{2fj}}{k_{fj}}$ is the ratio of species-2 diffusivity to thermal diffusivity, $\nu=\frac{\mu_{fj}}{\rho_{0fj}}$ is the kinematic viscosity and $d_{uf}=\frac{k_{fjT}\left(C_{1fj0}-C_{1fju}\right)}{k_{fj}\,(T_0-T_u)}$ is Dufour coefficient. For the porous layer, $p_{rm}=\frac{\phi\nu}{k_{mj}}$is the Prandtl number, $\beta^2{}_{mj}=\frac{K_{mj}}{d_{mj}^2}=D_a$ is the Darcy number, $\tau_{1mj}=\frac{k_{1mj}}{k_{mj}}$ is the ratio of species-1 diffusivity to thermal diffusivity, $\tau_{2mj}=\frac{k_{2mj}}{k_{mj}}$ is the ratio of species-2 diffusivity to thermal diffusivity, $d_{um}=\frac{k_{mjT}\left(C_{1mjL}-C_{1mj0}\right)}{k_{mj}\,(T_L-T_0)}$ is the Dufour coefficient and $\hat{\mu}=\frac{\mu_{mj}}{\mu_{fj}}$ is the viscosity ratio.

Boundary conditions

At the upper boundary,

$$W_{fj}(1)=0,\qquad D_{fj}\Theta_{fj}(1)=0,\ D_{fj}S_{1fj}(1)=0,\ D_{fj}S_{2fj}(1)=0,$$

$$W_{fj}(1)-M_{fj}a^2{}_{fj}\,\Theta_{fj}(1)-M_{sfj1}\,a^2{}_{fj}\,S_{fj}(1)=0$$

At the interface

$$W_{fj}(0)=\frac{\varsigma}{\varepsilon_T}W_{mj}(0),\qquad S_{1fj}(0)=\frac{\varepsilon_{1s}}{\varsigma}S_{1mj}(0),\ \Theta_{fj}(0)=\frac{\varepsilon_T}{\varsigma}\Theta_{mj}(0),$$

$$D_{fj}\Theta_{fj}(0)=D_{mj}\Theta_{mj}(0),\ D_{fj}S_{2fj}(0)=D_{mj}S_{2mj}(0), S_{1fj}(0)=\frac{\epsilon_{2s}}{\varsigma}S_{1mj}(0)$$

$$D_{fj}W_{fj}(0)=\frac{\varsigma^2}{\varepsilon_T}D_{mj}W_{mj}(0),\ D_{fj}S_{1fj}(0)=D_{mj}S_{1mj}(0)\left[D^3{}_{fj}-3a^2{}_{fj}\,D_{fj}\right]W_{fj}(0)$$
$$=\frac{-\varsigma^2}{D_a\varepsilon_T}D_{mj}W_{mj}(0)+\frac{\varsigma^4}{\varepsilon_T}\left[D_{mj}^3 3a_{mj}^2 D_{mj}\right]W_{mj}(0)$$

At the lower boundary

$$W_{mj}(-1)=0,\ D_{mj}W_{mj}(-1)=0,\ D_{mj}\Theta_{mj}(-1)=0,\quad D_{mj}S_{1mj}(-1)=0,$$

$$D_{mj}S_{2mj}(-1)=0$$

Where, $M=-\frac{\partial\sigma}{\partial T}\frac{(T_0-T_u)d_{fj}}{\mu\,k_{fj}}, M_s=-\frac{\partial\sigma}{\partial s}\frac{\left(C_{fj0}-C_{fju}\right)d_{fj}}{\mu\,k_{fj}}$ are the thermal and solute Marangoni numbers respectively. $\varepsilon_T=\frac{k_{fj}}{k_{fj1}}=\frac{1}{\tau_{fj}}$, $\varepsilon_{1s}=\frac{k_{mj}}{k_{mj1}}=\frac{1}{\tau_{1mj}}$, $\varepsilon_{2s}=\frac{k_{mj}}{k_{mj2}}=\frac{1}{\tau_{2mj}}$ are the ratios of salinity diffusivity to thermal diffusivity for both fluid and porous layers respectively and $\varsigma=\frac{d_{fj}}{d_{mj}}$ is the depth ratio.

Exact Solution Procedure and Eigenvalue Evaluation

Velocity distribution for fluid and porous layer

The final solutions of the differential equations (15) and (19) are not depend on $\Theta_{fj}\left(z_{fj}\right)$, $\Theta_{mj}(z_{mj})$, $S_{1mj}(z_{mj})$ and $S_{2mj}(z_{mj})$. The expressions for W_{fj} and W_{mj} are solved by using the velocity boundary conditions and are obtained as below,

$$W_{fj}(z_{fj}) = A_1 \begin{Bmatrix} [cosh(m_1\, z_{fj}) + C_2\, Sinh(m_1\;\; z_{fj})] + \\ [\, C_3\, cosh(m_2\, z_{fj}) + C_4\, Sinh(m_2\;\; z_{fj})] \end{Bmatrix}$$

And

$$W_{mj}(z_{mj}) = B_1 \cosh(a_{mj} z_{mj}) + B_2 \sinh(a_{mj} z_{mj}) + B_3\, \cosh(\delta z_{mj}) + B_4 \sinh(\delta z_{mj})$$

Where,

$$C_2 = \frac{-y_2\, y_7\, y_4}{y_3 y_8\, y_6} - \frac{y_5\, y_{10}}{\delta\, y_6\, Cosh[\delta]} - B_3 \left[\frac{y_1\, y_7\, y_4}{y_3 y_8\, y_6} - \frac{y_9\, y_4}{y_8\, y_6} + \frac{y_5\, y_4}{y_6\, \delta\, Cosh[\delta]}\right]$$

$$C_3 = B_3 \left(\frac{\varsigma\, y_1}{\epsilon_T\, y_3} + \frac{\varsigma}{\epsilon_T}\right) + \frac{\varsigma\, y_2}{\epsilon_T\, y_3} - 1, \qquad B_1 = B_3 \left(\frac{y_1}{y_3} + \frac{y_2}{y_3}\right)$$

$$C_4 = (-C_2\, Sinh[m_1] - C_3\, Cosh[m_2] - Cosh[m_1]) \left(\frac{1}{Sinh[m_2]}\right)$$

$$B_2 = -\frac{y_2\, y_7}{y_3\, y_8} - B_3 \left[\frac{y_1\, y_7}{y_3 y_8} - \frac{y_9}{y_8}\right], B_4 = -\frac{y_{11}\, B_3}{\delta\;\; Cosh[\delta]} - \frac{y_{10}}{\delta\;\; Cosh[\delta]}$$

$$B_3 = \frac{(y_1/y_3) - C_3 \left(\frac{\epsilon_T}{\varsigma}\right) - \left(\frac{\epsilon_T}{\varsigma}\right)}{1 - (y_1/y_3)}, y_1 = \frac{\varsigma}{\varepsilon T} - \frac{X_5}{X_3}, y_2 = \frac{X_2}{X_3} - 1, y_3 = \frac{X_4}{X_3} - \frac{\varsigma}{\varepsilon T}$$

$$y_4 = \frac{\varsigma^2 a_m x_9}{\varepsilon T} - m_2 X_{10}, \qquad y_5 = \frac{\varsigma^2 \delta x_9}{\varepsilon T} - m_2 X_{11}, \qquad y_6 = m_1 X_9 - m_2 X_8,$$

$$y_7 = \delta\, Cosh[\delta]\, Cosh[\, a_m] - a_m\, Sinh\, [a_m]\, Sinh[\delta],$$

$$y_8 = a_m Cosh[a_m] Sinh[\delta] - Sinh[a_m]\, \delta\, Cosh[\delta],$$

$$y_9 = \delta (Cosh[\delta])^2 - \delta (Sinh[\delta])^2,\; y_{10} = -\frac{a_m\, Sinh[a_m] y_2}{y_3} - \frac{a_m Cosh[a_m] y_2 y_7}{y_3 y_8}$$

$$y_{11} = -\frac{a_m Sinh[a_m] y_1}{y_3} - \frac{a_m Cosh[a_m] y_1 y_7}{y_3 y_8} + \frac{a_m Cosh[a_m] y_9}{y_8} - \delta\, Sinh[\delta]$$

$$y_{12} = -\frac{y_2 y_7 y_4}{y_3 y_8 y_6} - \frac{y_5 y_{10}}{\delta y_6\, Cosh[\delta]}, y_{13} = \frac{y_1 y_7 y_4}{y_3 y_8 y_6} - \frac{y_9 y_4}{y_8 y_6} + \frac{y_5 y_4}{y_6 \delta\, Cosh[\delta]}$$

Species-1 Concentration distribution for fluid and porous layer

The concentration distributions $S_{1fj}(z_{fj})$ and $S_{1mj}(z_{mj})$ are getting from the Differential Equations (17) and (21) by substituting the algebraic expressions for $W_{fj}(z_{fj})$ and $W_{mj}(z_{mj})$ and are solved using the concentration boundary conditions and are as below.

$$S_{1fj}(z_{fj}) = C_5\, \mathrm{Cosh}[a_{fj} z_{fj}] + C_6\, \mathrm{Sinh}[a_{fj}\, z_{fj}] + F_1(z_{fj}) + F_2(z_{fj})$$

And

$$S_{1mj}(z_{mj}) = B_6 \mathrm{Cosh}[a_{mj} z_{mj}] + B_7\, \mathrm{Sinh}[a_{mj} z_{mj}] + G_1(z_{mj}) + G_2(z_{mj})$$

Where,

ISSN No. 2454-6194 | DOI: 10.51584/IJRIAS |Volume XI Issue VII July 2026

$$F_1(z_{fj}) = -\frac{1}{\tau_1(m_1{}^2 - a_{fj}{}^2)}\left(Cosh[m_1\, z_{fj}] - C_2\, Sinh[m_1\, z_{fj}]\right)$$

$$F_2(z_{fj}) = -\frac{1}{\tau_1(m_2{}^2 - a_{fj}{}^2)}\left(\, C_3\, Cosh[m_2\, z_{fj}] - C_4\, Sinh[m_2\, z_{fj}]\right)$$

$$G_1(z_{mj}) = -\frac{z_m}{2a\tau_{1_p}}\left[B_2 Cosh[a_{mj}z_{mj}] + B_1 Sinh[a_{mj}z_{mj}]\right]$$

$$G_2(z_{mj}) = -\frac{B_3}{\tau_{1p}(\delta^2 - a^2)}Cosh[a_{mj}z_{mj}] - \frac{B_4}{\tau_{1_p}(\delta^2 - a^2)}Sinh[a_{mj}z_{mj}]$$

$$C_5 = \frac{\varepsilon_s}{\varsigma}B_6 + X_{3,}\;\; C_6 = \frac{1}{a_{fj}Cosh[a_{fj}]}[-X_5 B_6 - X_7],\;\;\; B_7 = \frac{a}{a_m}c_6 + X_4$$

$$B_6 = \frac{-a_{fj}\, Cosh[a_{mj}]X_7 + a_{fj}\, Cosh[a_{mj}]\, X_8}{[X_5\, a_{fj}\, Cosh[a_{mj}] + a_{fj}\, a_{mj}\, Cosh[a_{fj}]\, Sinh[a_{mj}]]}$$

$$X_3 = -\left(\frac{\varepsilon_{s1}}{\zeta}\right)\frac{B_3}{\tau_{1mj}(\delta^2 - a_{fj}^2)} + \frac{1}{\tau_{1fj}(m_1^2 - a_{fj}^2)} + \frac{C_3}{\tau_{1fj}(m_2^2 - a_{fj}^2)}$$

$$X_4 = -\frac{m_1 C_2}{\tau_{1fj}\, a_{mj}\,(m_1^2 - a_{fj}^2)} - \frac{m_2 C_4}{a_{mj}\,\tau_{1fj}\,(m_2^2 - a_{fj}^2)} + \frac{B_2}{2a_{fj}\tau_{1mj}a_{mj}} + \frac{B_4}{\tau_{1mj}(\delta^2 - a_{fj}^2)}$$

$$X_5 = \frac{a_{fj}\, Sinh[a_{fj}]\;\; \varepsilon_{s1}}{\zeta}, X_7 = a_{fj}\, Sinh[a_{fj}]\, X_3 - X_1, X_8 = a_{mj}Cosh[a_{mj}]\;\; X_4 + X_2$$

Species-2 Concentration distribution for fluid and porous layer

The concentration distributions $S_{2fj}(z_{fj})$ and $S_{2mj}(z_{mj})$ are getting from the Differential Equations (18) and (22) by substituting the algebraic expressions for $W_{fj}(z_{fj})$ and $W_{mj}(z_{mj})$ and are solved using the concentration boundary conditions and are as below.

$$S_{2fj}(z_{fj}S_{1fj}(z_{fj}) = C_{05}\,\mathrm{Cosh}[a_{fj}z_{fj}] + C_{06}\,\mathrm{Sinh}[a_{fj}\, z_{fj}] + F_{01}(z_{fj}) + F_{02}(z_{fj})$$

And

$$S_{1mj}(z_{mj}) = B_{06}\mathrm{Cosh}[a_{mj}z_{mj}] + B_{07}\,\mathrm{Sinh}[a_{mj}z_{mj}] + G_{01}(z_{mj}) + G_{02}(z_{mj})$$

Where,

$$F_1(z_{fj}) = -\frac{1}{\tau_1(m_1{}^2 - a_{fj}{}^2)}\left(Cosh[m_1\, z_{fj}] - C_2\, Sinh[m_1\, z_{fj}]\right)$$

$$F_2(z_{fj}) = -\frac{1}{\tau_1(m_2{}^2 - a_{fj}{}^2)}\left(\, C_3\, Cosh[m_2\, z_{fj}] - C_4\, Sinh[m_2\, z_{fj}]\right)$$

$$G_{01}(z_{mj}) = -\frac{z_m}{2a_{fj}\,\tau_{1mj}}\left[B_2 Cosh[a_{mj}z_{mj}] + B_1 Sinh[a_{mj}z_{mj}]\right]$$

$$G_{02}(z_{mj}) = -\frac{B_3}{\tau_{1mj}(\delta^2 - a_{fj}{}^2)}Cosh[a_{mj}z_{mj}] - \frac{B_4}{\tau_{1mj}(\delta^2 - a_{fj}{}^2)}Sinh[a_{mj}z_{mj}]$$

$$C_{05} = \frac{\varepsilon_{s2}}{\varsigma} B_6 + X_3, \; C_6 = \frac{1}{a_{fj} Cosh[a_{fj}]} [-X_5 B_6 - X_7], \quad B_7 = \frac{a_{fj}}{a_{mj}} C_{06} + X_4$$

$$B_6 = \frac{-a_{fj}\, Cosh[a_{mj}] X_7 + a_{fj}\, Cosh[a_{mj}]\, X_8}{[X_5\, a_{fj}\, Cosh[a_{mj}] + a_{fj}\, a_{mj}\, Cosh[a_{fj}]\, Sinh[a_{mj}]]}$$

$$X_3 = -\left(\frac{\varepsilon_{s2}}{\zeta}\right) \frac{B_3}{\tau_{2mj}(\delta^2 - a_{fj}^2)} + \frac{1}{\tau_{2fj}(m_1^2 - a_{fj}^2)} + \frac{C_3}{\tau_{2fj}(m_2^2 - a_{fj}^2)}$$

$$X_4 = -\frac{m_1 C_2}{\tau_{2fj}\, a_{mj}\, (m_1^2 - a_{fj}^2)} - \frac{m_2 C_4}{a_{mj}\, \tau_{2fj}\, (m_2^2 - a_{fj}^2)} + \frac{B_2}{2 a_{fj} \tau_{2mj} a_{mj}} + \frac{B_4}{\tau_{2mj}(\delta^2 - a_{fj}^2)}$$

$$X_5 = \frac{a_{fj}\, Sinh[a_{fj}]\;\; \varepsilon_{s1}}{\zeta}, X_7 = a_{fj}\, Sinh[a_{fj}]\, X_3 - X_1, X_8 = a_{mj} Cosh[a_{mj}]\;\, X_4 + X_2$$

Temperature distribution for fluid and porous layer

The temperature distributions$\Theta_{fj}(z_{fj})$ and $\Theta_{mj}(z_{mj})$are getting from the Differential Equations (18) and (22) by substituting the algebraic expressions$W_{fj}(z_{fj})$, $W_{mj}(z_{mj})$, $S_{fj}(z_{fj})$ and $S_{mj}(z_{mj})$ and are solved by the make use of temperature boundary conditions and are as follows .

$$\theta(z_{fj}) = C_7 Cosh[a_{fj}\, z_{fj}] + C_8 Sinh[a_{fj}\, z_{fj}] + F_5(z_{fj}) + F_6(z_{fj}) + F_7(z_{fj}) + F_8(z_{fj}) + F_9(z_{fj})$$

And

$$\theta_{mj}(z_{mj}) = B_8\, Cosh[a_{mj}\, z_{mj}] + B_9\, Sinh[a_{mj}\, z_{mj}] + F_3(z_{fj}) + F_4(z_{fj}) + F_{14}(z_{fj})$$

Where

$$F_5(z_{fj}) = -\frac{1}{m_1^2 - a^2{}_{fj}}\left(1 - \frac{Drm_1^2}{\tau_{1fj}(m_1^2 - a^2{}_{fj})} - \frac{Dra^2}{\tau_{1fj}(m_1^2 - a^2{}_{fj})}\right) Cosh[m_1\, z_{fj}]$$

$$F_6(z_{fj}) = -\frac{C_2}{m_1^2 - a^2{}_{fj}}\left(1 - \frac{Drm_1^2}{\tau_{1fj}(m_1^2 - a^2{}_{fj})} - \frac{Dra^2}{\tau_{1fj}(m_1^2 - a^2{}_{fj})}\right) Sinh[m_1\, z_{fj}]$$

$$F_7(z_{fj}) = -\frac{c_3}{m_2^2 - a^2{}_{fj}}\left(1 - \frac{Drm_2^2}{\tau_1(m_2^2 - a^2{}_{fj})} - \frac{Dra^2}{\tau_1(m_2^2 - a^2{}_{fj})}\right) Cosh[m_2\, z_{fj}]$$

$$F_8(z_{fj}) = -\frac{c_4}{m_2^2 - a^2{}_{fj}}\left(1 - \frac{Drm_2^2}{\tau_1(m_2^2 - a^2{}_{fj})} - \frac{Dra^2}{\tau_1(m_2^2 - a^2{}_{fj})}\right) Sinh[m_2\, z_{fj}]$$

$$F_9(z_{fj}) = d_{uf}\, z_{fj}\, (C_5 Sinh[a_{fj}\, z_{fj}] + C_6 Cosh[a_{fj}\, z_{fj}]$$

$$F_3(z_{fj}) = -\left(\frac{B_3}{\delta^2 - a_{mj}^2}\right) Cosh[\,\delta\, z_{mj}] - \left(\frac{B_4}{\delta^2 - a_{mj}^2}\right) Sinh[\,\delta\, z_{mj}]$$

$$F_4(z_{fj}) = \frac{z_{mj}}{2\, a_{mj}} (B_1\, Sinh[\, a_{mj}\, z_{mj}] + B_2\, Cosh[\, a_{mj}\, z_{mj}])$$

$$F_{10}(z_{fj}) = \frac{d_{um}\, a_{mj}}{2} (\, z_{mj}\, B_6\, Sinh[\, a_{mj}\, z_{mj}] + B_7\, Cosh[\, a_{mj}\, z_{mj}])$$

ISSN No. 2454-6194 | DOI: 10.51584/IJRIAS |Volume XI Issue VII July 2026

$$F_{11}(z_{fj}) = \frac{a_{mj}}{2\, a_{mj}\ \tau_{1mj}}\left(B_2\, Sinh[\, a_{mj}\, z_{mj}] + B_1\, Cosh[\, a_{mj}\, z_{mj}]\right)$$

$$F_{12}(z_{fj}) = \frac{z_{mj}}{2\, a_{mj}\ \tau_{1mj}}\left(B_1\, Sinh[\, a_{mj}\, z_{mj}] + B_2\, Cosh[\, a_{mj}\, z_{mj}]\right)$$

$$F_{13}(z_{fj}) = \frac{{a_{mj}}^2}{\tau_{1mj}(\delta^2 - a_{mj}^2)}\left(B_4\, Sinh[\, a_{mj}\, z_{mj}] + B_3\, Cosh[\, a_{mj}\, z_{mj}]\right)$$

$$F_{14}(z_{fj}) = F_{10}(z_{fj}) + F_{11}(z_{fj}) + F_{12}(z_{fj}) + F_{13}(z_{fj})$$

$$C_8 = \left(\frac{a_{mj}}{a_{fj}}\right)B_9 - \frac{X_{19}}{a_{fj}}\ , C_7 = -C_8 Sinh[a_{fj}] - \frac{X_{12}}{Cosh[a_{fj}]}\ , B_8 = \frac{a_m B_9 Cosh[a_{mj}] + X_{20}}{a_m Sinh[a_{mj}]}$$

$$X_{12} = L_9 + L_{10} + L_{11} + L_{12}$$

$$L_9 = -\frac{1}{m_1^2 - a_{fj}^2}\left(1 - \frac{d_{uf}\ m_1^2}{\tau_{1fj}(m_1^2 - a_{fj}^2)} - \frac{d_{uf}\ a_{fj}^2}{\tau_{1fj}(m_1^2 - a_{fj}^2)}\right) Cosh\ [m_1]$$

$$L_{10} = \frac{C_2}{m_1^2 - a_{fj}^2}\left(1 - \frac{d_{uf}\ m_1^2}{\tau_{1fj}(m_1^2 - a_{fj}^2)} - \frac{d_{uf}\ a_{fj}^2}{\tau_{1fj}\ (m_1^2 - a_{fj}^2)}\right) Snh\ [m_1]$$

$$L_{11} = -\frac{C_3}{m_2^2 - a_{fj}^2}\left(1 - \frac{d_{uf}\ m_2^2}{\tau_{1fj}\ (m_2^2 - a_{fj}^2)} - \frac{d_{uf}\ a_{fj}^2}{\tau_{1fj}\ (m_2^2 - a_{fj}^2)}\right) Cosh[m_2]$$

$$L_{12} = -\frac{C_4}{m_2^2 - a_{fj}^2}\left(1 - \frac{d_{uf}\ m_2^2}{\tau_{1fj}(m_2^2 - a_{fj}^2)} - \frac{d_{uf} a_{fj}^2}{\tau_{1fj}(m_2^2 - a_{fj}^2)}\right) Sinh[m_2]$$

$$L_{13} = d_{uf}(C_5 Sinha + C_6 Cosha)$$

$$B_9 = -\frac{X_{21}\ a_{mj}\ Sinh[a_{mj}] - X_{20}\ Cosh[a_{fj}]}{\left(\frac{a_{mj}^2}{a_{fj}}\right)\ Sinh[a_{fj}] Sinh[a_{mj}] + a_{mj}\ Cosh[a_{mj}]\ Cosh[a_{fj}]}$$

$$X_{19} = -\frac{\delta B_4}{(\delta^2 - a_{mj}^2)} + \frac{B_2}{2a_{mj}} + \frac{d_{um}\, a_{mj}\, B_7}{2} + \frac{a_{mj}^2\, B_2}{2a_{mj}\tau_{1mj}} + L_1$$

$$L_1 = \frac{B_2}{2a_m \tau_{1mj}} + \frac{B_4 a_{mj}^3}{\tau_{1mj}\ (\delta^2 - a_{mj}^2)} + m_1 X_{16} + m_2 X_{18} - d_{uf} C_6$$

$$X_{21`} = -Cosh[a_{fj}]X_{14} + Cosh[a_{fj}]X_{13} - X_{19}\left(\frac{Sinh[a_{fj}]}{a_{fj}}\right) + X_{12}$$

$$X_{20} = \frac{B_3 \delta}{\delta^2 - a_{mj}^2}\sinh[\delta] - \frac{\delta B_4}{\delta^2 - a_{mj}^2} - \frac{[a_{mj} B_1 \cosh[a_{mj}] - a_{mj} B_2 \sinh[a_{mj}]]}{2\mathrm{a_{mj}}} + L_5$$

$$L_5 = L_2 + L_3 + L_4 + L_6 + L_7 + L_8$$

$$L_7 = \frac{1}{2a_{mj}\tau_{1mj}}\left[-a_{mj}^2 B_1 \sinh[a_{mj}] + a_{mj}^2 B_2 \cosh[a_{mj}]\right]$$

ISSN No. 2454-6194 | DOI: 10.51584/IJRIAS |Volume XI Issue VII July 2026

$$L_8 = d_{um}\, a_{mj}\,\left(B_6\, a_{mj}\, Cosh\left[a_{mj}\right] - a_{mj}\, B_7\, Sinh[a_{mj}]\right)$$

$$L_6 = \frac{\left[-B_1 \sinh\left[a_{mj}\right] + B_2 \cosh\left[a_{mj}\right]\right]}{2a_{mj}} + \frac{d_{um}\, a_{mj}\left[-B_6 \sinh\left[a_{mj}\right] + B_7 \cosh\left[a_{mj}\right]\right]}{2}$$

$$L_4 = \frac{a_{mj}^2}{\tau_{1mj}\left(\delta^2 - a_{mj}^2\right)\left[-a_{mj}B_3 \sinh\left[a_{mj}\right] + B_4 a_{mj} \cosh\left[a_{mj}\right]\right]}$$

$$L_2 = -\frac{1}{2a_{mj}\tau_{1mj}}\left[B_2 \cosh\left[a_{mj}\right] - B_1 \sinh\left[a_{mj}\right]\right]$$

$$L_3 = \frac{\left[-a_m B_2 \sinh\left[a_{mj}\right] + a_{mj}\mathrm{B}_1 \cosh\left[a_{mj}\right]\right]}{2a_{mj}\tau_{1mj}}$$

To obtain the Eigenvalue, the thermal Marangoni number

The thermal Marangoni number is obtained by using the coupled boundary condition at the upper fluid boundary which is free with Marangoni effects, which is

$$D_{fj}^2\, W_{fj}(1) - Ma_{fj}^2\Theta_{fj}(1) - M_{sf1}\, a_{fj}^2 S_{fj}(1) - M_{sf2}\, a_{fj}^2 S_{fj}(1) = 0$$

By solving for M, by substituting all the known quantities, we get

$$M = \frac{\psi_1 - M_{sf1}\, a_{fj}^2\ \psi_2 - M_{sf2}\, a_{fj}^2\ \psi_4}{a_{fj}^2\, \psi_3}$$

Where,

$$\psi_1 = m_1^2\, Cosh[m_1] + C_2 m_1^2\, Sinh[m_1] + C_3 m_2^2\, Cosh[m_2] + C_4 m_2^2\, Sinh[m_2]$$

$$\psi_2 = C_5\, Cosh\left[a_{fj}\right] + C_6\, Sinh\left[a_{fj}\right] - \frac{Cosh[m_1]}{\tau_{1fj}\left(m_1^2 - a_{fj}^2\right)} - \frac{C_2 Sinh[m_1]}{\tau_{1fj}\left(m_1^2 - a_{fj}^2\right)} + L_{14}$$

$$L_{14} = -\frac{C_3 Cosh[m_2]}{\tau_{1fj}\left(m_2^2 - a_{fj}^2\right)} - \frac{C_4 Sinh[m_2]}{\tau_{1fj}\left(m_2^2 - a_{fj}^2\right)}$$

$$\psi_3 = C_7 Cosha + C_8 Sinha + L_{15} + L_{16} + L_{17} + L_{18} + L_{19}$$

$$\psi_4 = C_7 Cosha + C_8 Sinha + L_{20} + L_{21} + L_{22} + L_{23} + L_{24}$$

$$L_{15} = -\frac{1}{m_1^2 - a_{fj}^2}\left(1 - \frac{d_{uf}\, m_1^2}{\tau_{1\mathrm{fj}}\left(m_1^2 - a_{fj}^2\right)} - \frac{d_{uf}\, a^2}{\tau_{1\mathrm{fj}}\left(m_1^2 - a_{fj}^2\right)}\right) Cosh[m_1]$$

$$L_{16} = -\frac{c_2}{m_1^2 - a_{fj}^2}\left(1 - \frac{d_{uf}\, m_1^2}{\tau_{1\mathrm{fj}}\left(m_1^2 - a_{fj}^2\right)} - \frac{d_{uf}\, a^2}{\tau_{1\mathrm{fj}}\left(m_1^2 - a_{fj}^2\right)}\right) Sinh[m_1]$$

$$L_{17} = -\frac{c_3}{m_2^2 - a_{fj}^2}\left(1 - \frac{d_{uf}\, \mathrm{m}_2^2}{\tau_{1fj}\left(m_2^2 - a_{fj}^2\right)} - \frac{d_{uf} a^2}{\tau_{1\mathrm{fj}}\left(m_2^2 - a_{fj}^2\right)}\right) Cosh[m_2]$$

$$L_{18} = -\frac{c_4}{m_2^2 - a_{fj}^2}\left(1 - \frac{d_{uf}\, m_2^2}{\tau_{1fj}\left(m_2^2 - a_{fj}^2\right)} - \frac{d_{uf}\, a^2}{\tau_{1fj}\left(m_2^2 - a_{fj}^2\right)}\right) Sinh[m_2]$$

$$L_{19} = d_{uf}\left(C_5\, Sinh\left[a_{fj}^2\right] + C_6\, Cosh\left[a_{fj}^2\right]\right)$$

$$L_{20} = -\frac{1}{m_1^2 - a_{fj}^2}\left(1 - \frac{d_{uf}\, m_1^2}{\tau_{2\mathrm{fj}}\left(m_1^2 - a_{fj}^2\right)} - \frac{d_{uf}\, a^2}{\tau_{2\mathrm{fj}}\left(m_1^2 - a_{fj}^2\right)}\right) Cosh[m_1]$$

$$L_{21} = -\frac{c_2}{m_1^2 - a_{fj}^2}\left(1 - \frac{d_{uf}\, m_1^2}{\tau_{2\mathrm{fj}}\left(m_1^2 - a_{fj}^2\right)} - \frac{d_{uf}\, a^2}{\tau_{2\mathrm{fj}}\left(m_1^2 - a_{fj}^2\right)}\right) Sinh[m_1]$$

$$L_{22} = -\frac{c_3}{m_2^2 - a_{fj}^2}\left(1 - \frac{d_{uf}\, \mathrm{m}_2^2}{\tau_{2fj}\left(m_2^2 - a_{fj}^2\right)} - \frac{d_{uf} a^2}{\tau_{2\mathrm{fj}}\left(m_2^2 - a_{fj}^2\right)}\right) Cosh[m_2]$$

$$L_{23} = -\frac{c_4}{m_2^2 - a_{fj}^2}\left(1 - \frac{d_{uf}\, m_2^2}{\tau_{2fj}\left(m_2^2 - a_{fj}^2\right)} - \frac{d_{uf}\, a^2}{\tau_{2fj}\left(m_2^2 - a_{fj}^2\right)}\right) Sinh[m_2]$$

$$L_{24} = d_{uf}\,\left(C_5\, Sinh\left[a_{fj}^2\right] + C_6\, Cosh\left[a_{fj}^2\right]\right.$$

Graphical Results and Quantitative Interpretation

The thermal Marangoni number (M), which serves as the eigenvalue of the stability problem for non-Darcy three-component Marangoni convection with combined Dufour and magnetic effects in a two-layer composite system, is obtained in closed form as a function of several governing physical parameters. These parameters include the Darcy number, the ratio of diffusivities, the viscosity ratio, the Dufour parameters, the magnetic parameter, the concentration ratios, and the depth ratio of the two layers.

To analyze the influence of these parameters on the stability characteristics of the system, the eigenvalue corresponding to the thermal Marangoni number is plotted as a function of the depth ratio for various values of the other physical parameters. The graphical results provide insight into the effects of magnetic field strength, Dufour effects, permeability variations, and diffusivity ratios on the onset of convection and the stability behaviour of the composite system.

Figure 1 illustrates the variation of the thermal Marangoni number M with the horizontal wave number. It is observed that an increase in the horizontal wave number raises the critical thermal Marangoni number, indicating that the system becomes more stable. Physically, larger wave numbers correspond to smaller convection cells, which experience stronger viscous and diffusive damping effects. Therefore, a larger thermal driving force is required to initiate convection. This stabilising influence of wave number is consistent with the classical Marangoni convection analysis of Pearson (1958), who showed that short wavelength disturbances require higher critical Marangoni numbers for instability. Similar observations were also reported by Nield and Bejan (2017) in porous medium convection systems and by Rudraiah et al. in studies of surface-tension-driven convection in composite layers.

Figure 2 depicts the effect of the Darcy number on the thermal Marangoni number M. The Darcy number measures the permeability of the porous medium. As the Darcy number increases, the resistance offered by the porous structure decreases, allowing fluid particles to move more freely. Consequently, convection is promoted at lower thermal gradients, leading to a decrease in the critical thermal Marangoni number and thereby destabilising the system. This physical behaviour agrees with the classical porous medium convection results of Lapwood (1948), who demonstrated that increasing permeability enhances convective motion. Similar destabilising effects of the Darcy number were also reported in Darcy–Brinkman convection studies by Vafai and Tien (1981) and in multilayer porous convection analyses by Shivakumara and co-workers.

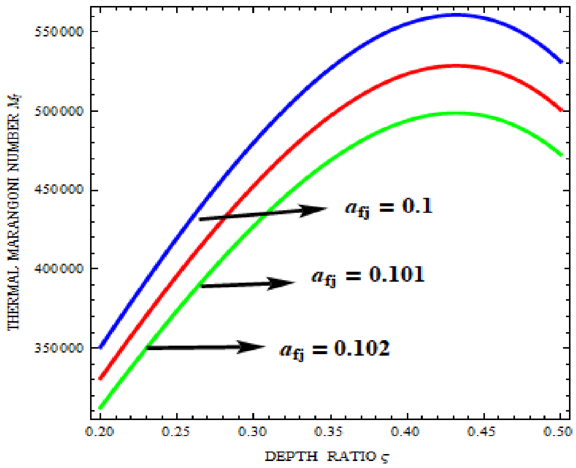

Figure 1: Impact of horizontal wave number a_{fj} on Thermal Marangoni number M

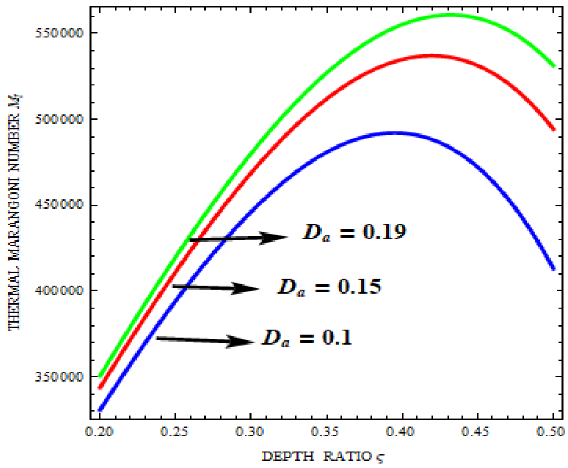

Figure 2: Impact of Darcy number D_a on Thermal Marangoni number M

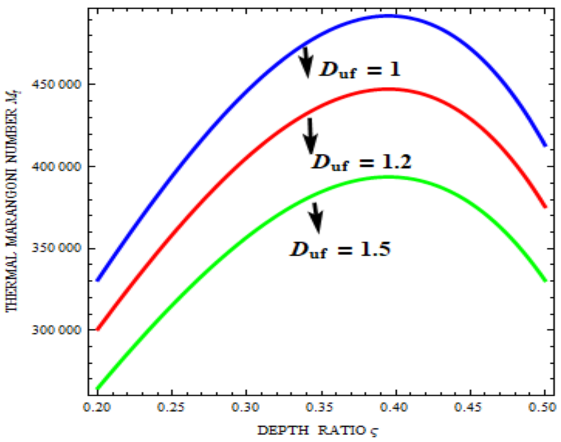

Figure 3: Impact of the Dufour number of the fluid layer D_{uf} on Thermal Marangoni number M

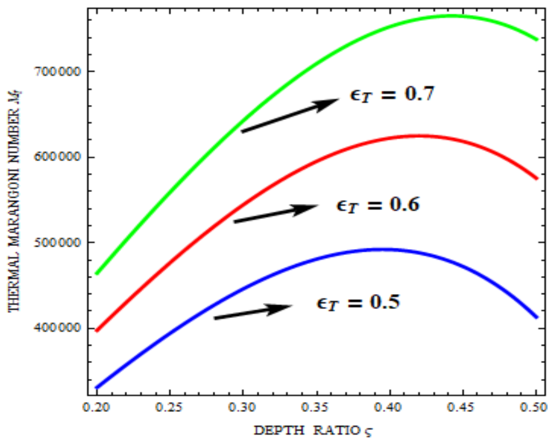

Figure 4: Impact of the ratio of Thermal solutal diffusivities in the fluid layer ϵ_T on Thermal Marangoni number M

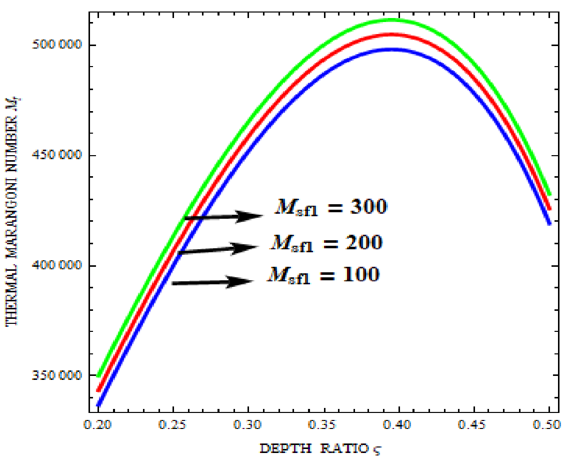

Figure 5: Impact of Solutal-1 Marangoni number M_{sf1} on Thermal Marangoni number M

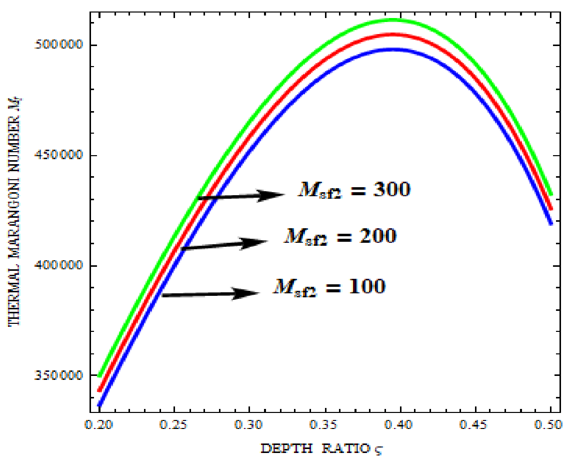

Figure 6: Impact of Solutal-2 Marangoni number M_{sf2} on Thermal Marangoni number M

ISSN No. 2454-6194 | DOI: 10.51584/IJRIAS |Volume XI Issue VII July 2026

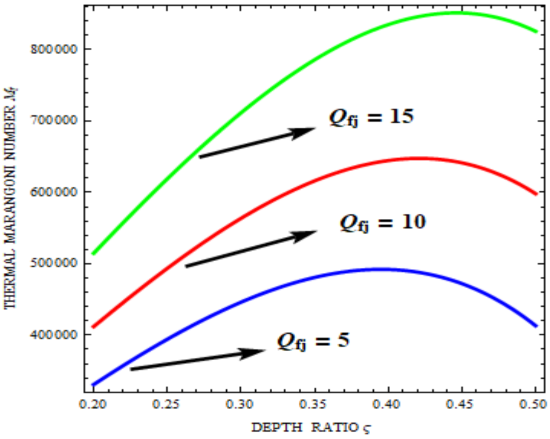

Figure 7: Impact of Chandrashekar number Q_{fj} of fluid layer on the Thermal Marangoni number M

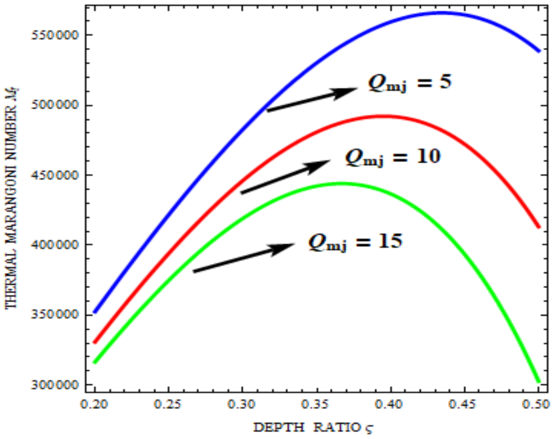

Figure 8: Impact of Chandrashekar number Q_{mj} of porous layer on the Thermal Marangoni number M

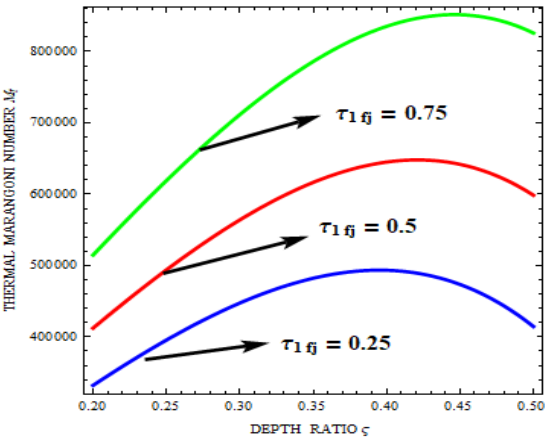

Figure 9: Impact of the ratio of solutal diffusivity to thermal diffusivity τ_{1fj} of the fluid layer on the Thermal Marangoni number M

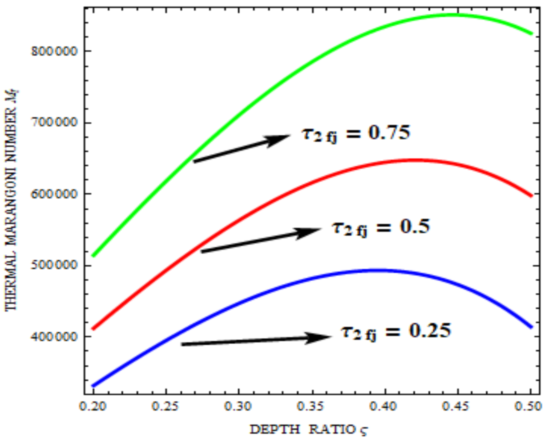

Figure 10: Impact of the ratio of solutal diffusivity to thermal diffusivity τ_{2fj} of fluid layer on the Thermal Marangoni number M

Figure 3 represents the influence of the Dufour number on the thermal Marangoni number M. The Dufour effect accounts for energy flux generated by concentration gradients and represents an important cross-diffusion phenomenon in multicomponent systems. An increase in the Dufour number enhances heat transport induced by concentration differences, thereby modifying the thermal energy distribution within the fluid layer. This additional heat flux alters the interfacial temperature gradients and consequently changes the surface tension forces responsible for Marangoni convection. The graphical results indicate that stronger Dufour effects significantly influence the onset of convection and modify the stability threshold of the system. Similar behavior has been reported in double-diffusive convection studies by Postelnicu (2004), where Dufour effects altered thermal instability characteristics in porous media. Srinivas Acharya and Kaladhar (2012) also observed that increasing Dufour effects considerably modify heat transfer and stability behavior in convection through porous layers. Comparable conclusions were obtained by Chamkha and Rashad (2014) in magnetohydrodynamic mixed convection flows with Soret and Dufour effects.

Figure 4 illustrates the effect of the ratio of thermal-solutal diffusivities on the thermal Marangoni number M. This parameter determines the relative rates of heat diffusion and mass diffusion within the composite system. Increasing the diffusivity ratio causes concentration gradients to dissipate more rapidly compared to thermal gradients, thereby weakening concentration-induced surface tension effects. As a result, convection is delayed, and the system exhibits enhanced stability. Physically, stronger thermal diffusion smoothens temperature variations and suppresses the growth of instability modes. Similar stabilising behaviour due to diffusivity variations was reported in thermosolutal convection studies by Nield (1968) and later by Poulikakos in multicomponent convection analyses. Comparable results were also observed in triple-diffusive convection studies involving layered systems.

Figure 5 shows the influence of the Solutal-1 Marangoni number on the thermal Marangoni number M. Increasing the Solutal-1 Marangoni number intensifies the concentration-induced surface tension gradients associated with the first solute component. This enhances interfacial shear stresses and promotes fluid motion near the interface, leading to earlier onset of convection. Consequently, the system becomes more unstable. Physically, concentration gradients act as an additional driving force that supplements thermal surface tension effects. Similar destabilizing effects of solutal Marangoni forces were reported by Sternling and Scriven (1959) in their classical thermocapillary instability analysis. Related observations were also made in multicomponent convection studies by Bergman and Keller.

Figure 6 depicts the variation of the thermal Marangoni number $M$with the Solutal-2 Marangoni number. Similar to the first solutal component, the second solute contributes to concentration-driven surface tension variations at the interface. Increasing the Solutal-2 Marangoni number strengthens the interfacial concentration gradients and enhances thermosolutal convection. This reduces the critical thermal Marangoni number and destabilises the system. The interaction between the two solutal components produces complex instability characteristics that are typical of three-component convection systems. Similar coupled solutal effects were discussed in the triple-diffusive convection studies of Pearlstein et al. and in multicomponent Marangoni instability analyses by Nepomnyashchy and Simanovskii.

Figure 7 illustrates the influence of the Chandrasekhar number $Q_f$of the fluid layer on the thermal Marangoni number M. The Chandrasekhar number represents the strength of the applied magnetic field. It is observed from the graph that increasing $Q_f$increases the critical thermal Marangoni number, thereby stabilising the system. Physically, the application of a magnetic field generates Lorentz forces within the electrically conducting fluid, which oppose fluid motion and suppress convective disturbances. This magnetic damping effect reduces the growth rate of instability and delays the onset of convection. Consequently, stronger thermal gradients are required to initiate Marangoni convection. Similar stabilising effects of magnetic fields have been reported in hydromagnetic convection studies by Chandrasekhar (1961) and later in magneto-Marangoni convection analyses by Rudraiah et al. and Gupta et al., where magnetic fields were shown to suppress surface-tension-driven instabilities in porous and composite systems.

Figure 8 depicts the effect of the Chandrasekhar number Q_{mj} of the porous layer on the thermal Marangoni number M. It is evident that increasing the magnetic parameter in the porous layer also increases the critical thermal Marangoni number, indicating stabilisation of the composite system. Physically, the magnetic field interacts with the electrically conducting fluid inside the porous matrix and generates resistive Lorentz forces that damp fluid motion. In porous media, this damping becomes more significant because the magnetic field acts together with the drag resistance of the porous structure. As a result, convective motion is strongly suppressed, and larger thermal gradients are needed to destabilise the system. Similar observations were reported in the magneto-porous convection studies of Nield and Bejan (2017) and in MHD Darcy–Brinkman convection analyses by Vafai and Tien (1981), where magnetic effects were found to significantly delay the onset of convection.

Figure 9 shows the impact of the ratio of solutal diffusivity to thermal diffusivity τ_{1fj} of the fluid layer on the thermal Marangoni number M. The parameter τ_{1fj} governs the relative diffusion rates of concentration and temperature fields in the fluid layer. It is observed that increasing τ_{1fj} increases the thermal Marangoni number, indicating a stabilising influence on the system. Physically, larger values of τ_{1fj} correspond to stronger solutal diffusion, which smoothens concentration gradients more rapidly and weakens concentration-induced surface tension forces at the interface. This suppresses thermosolutal convection and delays the onset of instability. Similar stabilising behaviour due to enhanced diffusivity ratios has been reported in double-diffusive and triple-diffusive convection studies by Poulikakos (1985) and Pearlstein et al. (1989), where increased mass diffusivity reduced concentration-driven instabilities.

Figure 10 illustrates the influence of the ratio of solutal diffusivity to thermal diffusivity τ_{2fj} of the fluid layer on the thermal Marangoni number M. Similar to τ_{1fj}, increasing τ_{2fj} enhances the diffusion of the second solutal component relative to heat diffusion. As the concentration gradients dissipate more rapidly, the associated concentration-induced surface tension gradients become weaker, thereby stabilising the system. Consequently, higher thermal Marangoni numbers are required to trigger convection. The results indicate that the second solutal component plays an important role in controlling the thermosolutal instability of the three-component composite system. Similar conclusions were obtained in multicomponent convection analyses by Sternling and Scriven (1959) and in triple-diffusive instability studies by Rionero (1997), where enhanced solutal diffusivity was shown to suppress interfacial instability mechanisms.

CONCLUSIONS

The stability behaviour of non-Darcy three-component Marangoni convection with combined Dufour and magnetic effects in a two-layer composite system has been studied. From the analytical and graphical results, the following conclusions are obtained:

1. Increasing the horizontal wave number increases the thermal Marangoni number (M), which stabilises the system and delays the onset of convection.

2. Increasing the Darcy number decreases the thermal Marangoni number, thereby destabilising the system due to increased permeability of the porous medium.

3. The Dufour effect significantly affects the stability of the system by modifying heat transfer through concentration gradients.

4. Increasing the ratio of thermal-solutal diffusivities stabilises the system because concentration gradients diffuse more rapidly.

5. Increasing the Solutal-1 and Solutal-2 Marangoni numbers destabilises the system by strengthening concentration-induced surface tension forces.

6. The Chandrasekhar numbers of both the fluid and porous layers stabilise the system due to the magnetic damping effect produced by Lorentz forces.

7. Increasing the ratios of solutal diffusivity to thermal diffusivity τ_{1fj} and τ_{2fj} delays convection and enhances stability.

8. The combined effects of magnetic field, Dufour effect, porous medium permeability, and multicomponent diffusion strongly influence the onset of Marangoni convection.

9. The obtained results are in good agreement with previously published works on Marangoni convection, porous medium convection, and magnetohydrodynamic instability.

10. The present study is useful in understanding convection phenomena in applications such as crystal growth, geothermal systems, chemical engineering processes, and material processing involving multicomponent transport.

REFERENCES

1. Bejan, A., & Nield, D. A. (2017). Convection in porous media (5th ed.). Springer.
2. Bergman, T.L. and Keller, K.H. (1983). Combined buoyancy and thermocapillary convection in multilayer systems. Journal of Fluid Mechanics.
3. Chamkha, A. J., & Rashad, A. M. (2013). Unsteady natural convection from a vertical cylinder embedded in a porous medium with heat generation/absorption. International Journal of Thermal Sciences, 65, 58–67. https://doi.org/10.1016/j.ijthermalsci.2012.09.008

4. Chamkha, A.J. and Rashad, A.M. (2014). Unsteady heat and mass transfer by MHD mixed convection flow with Soret and Dufour effects past a stretching surface embedded in a porous medium. Journal of Applied Fluid Mechanics, 7(2), 263–272.
5. Chandrasekhar, S. (1961). Hydrodynamic and hydromagnetic stability. Oxford University Press.
6. Ghosh, S. K., & Mukherjee, S. (2021). Non-Darcy effects on thermal instability in porous media. Journal of Porous Media, 24(3), 45–62.
7. Gupta, A.S. and Sharma, V. (2004). Effect of magnetic field on Marangoni convection. International Journal of Engineering Science.
8. Kuznetsov, A. V. (2022). Triple-diffusive convection in nanofluid-saturated porous media. International Communications in Heat and Mass Transfer, 130, 105820. https://doi.org/10.1016/j.icheatmasstransfer.2021.105820
9. Lapwood, E.R. (1948). Convection of a fluid in a porous medium. Proceedings of the Cambridge Philosophical Society, 44, 508–521.
10. Nepomnyashchy, A.A. and Simanovskii, I.B. (2013). Convective instabilities in liquid and gas systems. CRC Press.
11. Nield, D.A. (1968). Surface tension and buoyancy effects in cellular convection. Journal of Fluid Mechanics, 19, 341–352.
12. Nield, D. A., & Kuznetsov, A. V. (2019). The onset of convection in a porous medium with a vertical magnetic field. Transport in Porous Media, 128, 1–20.
13. Pearson, J.R.A. (1958). On convection cells induced by surface tension. Journal of Fluid Mechanics, 4, 489–500.
14. Pearlstein, A.J., Harris, R.M., and Terrones, G. (1989). The onset of convective instability in a triply diffusive fluid layer. Journal of Fluid Mechanics, 202, 443–465.
15. Postelnicu, A. (2004). Influence of a magnetic field on heat and mass transfer by natural convection from vertical surfaces in porous media considering Soret and Dufour effects. International Journal of Heat and Mass Transfer, 47, 1467–1472.
16. Poulikakos, D. (1985). Double diffusive convection in fluid layers. International Journal of Heat and Mass Transfer.
17. Pranesh, S., & Kiran, A. (2020). Magnetohydrodynamic effects on double diffusive convection in porous media. Applied Mathematics and Mechanics, 41(5), 673–690.
18. Rionero, S. (1997). Triple diffusive convection in porous media. Acta Mechanica.
19. Rionero, S. (2021). Stability of convection in composite fluid–porous systems. Continuum Mechanics and Thermodynamics, 33, 1125–1142.
20. Rudraiah, N., et al. (1985). Surface tension driven convection in layered fluid systems. Acta Mechanica.
21. Rudraiah, N., Malashetty, M.S., and Shivakumara, I.S. (1987). Magnetoconvection in porous media. Acta Mechanica.
22. Shivakumara, I.S. and Rudraiah, N. (2002). Magneto-Marangoni convection in porous layers. Transport in Porous Media.
23. Shivakumara, I.S., et al. (2011). Marangoni convection in porous layers. Transport in Porous Media.
24. Siddheshwar, P. G., et al. (2019). Marangoni convection with thermosolutal effects. International Journal of Heat and Mass Transfer, 140, 123–135.
25. Srinivasacharya, D. and Kaladhar, K. (2012). Soret and Dufour effects on mixed convection flow in a non-Darcy porous medium saturated with nanofluid. Journal of Heat Transfer, 134(5), 052601.
26. Sternling, C.V. and Scriven, L.E. (1959). Interfacial turbulence: hydrodynamic instability and the Marangoni effect. AIChE Journal, 5, 514–523.
27. Vafai, K. and Tien, C.L. (1981). Boundary and inertia effects on flow and heat transfer in porous media. International Journal of Heat and Mass Transfer, 24, 195–203.
28. Zhao, L., Wang, Y., & Liu, H. (2024). Dufour and Soret effects in multicomponent convection systems. Physics of Fluids, 36(2), 024108.